

Influence of anode pore forming additives on the densification of supported $\text{BaCe}_{0.7}\text{Ta}_{0.1}\text{Y}_{0.2}\text{O}_{3-\delta}$ electrolyte membranes based on a solid state reaction

Lei Bi^a, Shumin Fang^{a,b}, Zetian Tao^a, Shangquan Zhang^a, Ranran Peng^a, Wei Liu^{a,*}

^a *Laboratory of Advanced Functional Materials and Devices, Department of Materials Science and Engineering, University of Science and Technology of China, Hefei, Anhui 230026, PR China*

^b *Inorganic Membranes, Faculty of Science and Technology and MESA+ Institute, University of Twente, P.O. Box 217, 7500 AE Enschede, The Netherlands*

Received 15 August 2008; received in revised form 17 February 2009; accepted 25 February 2009

Available online 25 March 2009

Abstract

We describe a solid state reaction for the preparation of both $\text{NiO-BaCe}_{0.7}\text{Ta}_{0.1}\text{Y}_{0.2}\text{O}_{3-\delta}$ anode substrates and $\text{BaCe}_{0.7}\text{Ta}_{0.1}\text{Y}_{0.2}\text{O}_{3-\delta}$ (BCTY10) electrolyte membranes on porous NiO-BCTY10 anode substrates. The amounts of the pore forming additive in the substrates showed a significant influence on the densification of the BCTY10 membranes. After sintering at 1450°C for 5 h, the BCTY10 membrane on a NiO-BCTY10 anode containing 30 wt.% starch achieved a high density and showed adequate chemical stability against H_2O and CO_2 . The chemical stability of BCTY10 was even better than that of $\text{BaCe}_{0.7}\text{Zr}_{0.1}\text{Y}_{0.2}\text{O}_{3-\delta}$. With a mixture of $\text{BaCe}_{0.7}\text{Zr}_{0.1}\text{Y}_{0.2}\text{O}_{3-\delta}$ (BZCY7) and $\text{La}_{0.7}\text{Sr}_{0.3}\text{FeO}_{3-\delta}$ (LSF) as a cathode, a single fuel cell with $12\ \mu\text{m}$ thick BCTY10 electrolyte generated maximum power densities of 142, 93, 29 mW/cm^2 at 700, 600 and 500°C , respectively. The electrolyte resistance and interfacial polarization resistance of the cell under open circuit conditions were also investigated.

© 2009 Elsevier Ltd. All rights reserved.

Keywords: Sintering; Solid state reaction; Fuel cell; Membranes; Pore forming additive

1. Introduction

Ceramic proton conductors have received much attention from the solid oxide fuel cell (SOFC) community because proton-conducting SOFCs would permit a reduction of the working temperature to the range $500\text{--}700^\circ\text{C}$.^{1–5} In addition, unlike conventional SOFCs with YSZ electrolyte, no circulation of fuel gas is necessary for proton-conducting SOFCs, as water is produced at the cathode side. Among these ceramic proton conductors, considerable attention has been paid to ABO_3 -type perovskites, particularly rare earth doped BaCeO_3 materials, which exhibit the highest protonic conductivities. Various processing techniques have been used for producing the doped BaCeO_3 thin film electrolytes in order to reduce the electrolyte resistance and improve cell performance, such as suspension spray,⁶ co-pressing,⁷ spin coating⁸ and screen printing.⁹ The majority has been proved to be suitable for laboratory demon-

stration but may present difficulties for mass production because the doped BaCeO_3 powders are usually needed to be prepared by a wet chemical route. This wet chemical process has complicated processing steps and high processing costs though ceramic powder prepared by a wet chemical process has better sintering activity. In addition, the solid state reaction has the advantages of simple processing steps and lower costs, which can fit the requirements for commercialization. However, the powders prepared by solid state reaction show lower sintering activity due to the high calcination temperatures used. In recent studies, an in situ solid state reaction method has been successfully used to prepare dense ceramic membranes on porous substrates.^{6,10–13} However, ceramic powders with high sintering activity (powders prepared through a wet chemical route⁶ or nano-sized ceramic powders¹²) are usually required to prepare the anode substrate, in order to maintain high sintering activity for the substrate. This can still hinder the commercialization of proton-conducting SOFCs because of the relatively high processing costs. Recently, Meulenberg et al.¹¹ have successfully used conventional techniques and materials to prepare proton-conducting electrolytes on standard anodes, which shed light on the manufacture of

* Corresponding author. Tel.: +86 551 3606929; fax: +86 551 3601592.
E-mail address: wliu@ustc.edu.cn (W. Liu).

SOFCs. As for mass production, it is necessary to find a simple route for preparing SOFCs based solely on a solid state reaction.

Another challenge for rare earth doped BaCeO_3 materials is the poor chemical stability of BaCeO_3 , which makes them inadequate for fuel cell applications.¹⁴ In order to solve this problem, much attention has been paid to the preparation of chemically stable ceramic proton conductors. The most widely used approach is the partial replacement of Ce by Zr at the cost of reducing the protonic conductivity, in order to seek a proper compromise between the conductivity and chemical stability.¹⁴ However, some investigations show that only BaCeO_3 -based materials with high doping concentrations of Zr can produce adequate chemical stability against H_2O and CO_2 .^{14,15} In addition, the high sintering temperature for the Zr-doped BaCeO_3 materials is another challenge for their practical use. Therefore, it is necessary to find alternative strategies for improving the chemical stability of BaCeO_3 . In our previous research,¹⁶ we have found that doping with a small amount of Ta can greatly increase the stability of the BaCeO_3 -based material. However, a wet chemical route for preparing the fuel cell is necessary, which may not fit the requirement of mass production. Furthermore, no direct comparison between the chemical stability of the commonly used Zr-doped BaCeO_3 and the Ta-doped BaCeO_3 has been made.

In this study, the stable $\text{BaCe}_{0.7}\text{Ta}_{0.1}\text{Y}_{0.2}\text{O}_{3-\delta}$ (BCTY10) electrolyte membranes have been successfully fabricated on porous NiO–BCTY10 anode substrates using a solid state reaction. We aim to study the influence of the amounts of the anode pore forming additive on the densification of the anode-supported BCTY10 membranes as well as the electrochemical properties of the BCTY10-based fuel cell.

2. Experimental

The NiO–BCTY10 anode substrates were prepared by directly mixing the metal oxides (NiO, BaCO_3 , CeO_2 , Y_2O_3 and Ta_2O_5) in appropriate proportions to make sure that the BCTY10 composition was $\text{BaCe}_{0.7}\text{Ta}_{0.1}\text{Y}_{0.2}\text{O}_{3-\delta}$ and the weight ratio of BCTY10:NiO was 4:6. Different amounts of starch (10, 20 and 30 wt.%) were added as the pore former. The mixed powders were pressed under a pressure of 200 MPa into disks 15 mm in diameter and 0.8 mm thick. These as-prepared green anode substrates containing different amounts of pore forming additive were stored ready for use. For comparison, another anode substrate containing the BCTY10 powder synthesized by a conventional solid state reaction process was prepared. In the conventional solid state reaction process, appropriate amounts of BaCO_3 , CeO_2 , Y_2O_3 and Ta_2O_5 were mixed and ball-milled in alcohol for 24 h. The mixture was then dried and calcined at 950, 1200 and 1400 °C for 5 h with intermittent grinding in an agate mortar. 30 wt.% starch was added as the pore former in this anode.

The BCTY10 membranes were fabricated on the anode substrates by an in situ reaction. The starting materials BaCO_3 , CeO_2 , Y_2O_3 and Ta_2O_5 were mixed in the molar ratio 1:0.7:0.1:0.05 and dispersed into ethanol by ball-milling for 24 h to form a suspension. The well-mixed suspension was directly

deposited on the anode substrate by a suspension spray method. The suspension was fluidized by a flow of air and sprayed on to the anode substrates, which rested on a heating plate during this process. Then the bi-layers of green electrolyte and anode were co-fired at 1450 °C in air for 5 h. A mixture of $\text{BaCe}_{0.7}\text{Zr}_{0.1}\text{Y}_{0.2}\text{O}_{3-\delta}$ (BZCY7) and $\text{La}_{0.7}\text{Sr}_{0.3}\text{FeO}_{3-\delta}$ (LSF) was printed on the dense anode-supported BCTY10 membrane electrolyte and then fired at 1000 °C for 3 h to form a porous cathode. The electrode active area was 0.237 cm². Pt paste was applied to the electrode as a current collector.

Powder X-ray diffraction measurements were made using a Philips X'Pert Pro Super diffractometer with Cu K α radiation. The shrinkage behaviors of the green anode substrates from room temperature to 1450 °C were measured with a thermal expansion analyzer (DIL 402C, NETZSCH). Electrochemical measurements on the fuel cell were performed in an Al_2O_3 test housing placed inside a furnace. Humidified hydrogen (~3% H_2O) was fed to the anode chamber at a flow rate of 25 mL/min while the cathode was exposed to atmospheric air. The anode side was sealed with Ag paste. Fuel cell performance was measured with a DC Electronic Load apparatus (ITech Electronics model IT8511). Resistances of the cell under open circuit conditions were measured at different temperatures by an impedance analyzer (CHI604C, Chenhua Inc., Shanghai). A 5 mV A.C. signal was applied and the frequency was swept from 100 KHz to 0.1 Hz. A scanning electron microscope (SEM, JEOL JSM-6700F) was used to observe the fracture morphologies of the BCTY10 membranes and the tested cell.

3. Results and discussion

We know that the high shrinkage of an anode substrate can promote the densification of a supported electrolyte membrane during the co-firing process. Fig. 1 shows the shrinkage behavior of the anode substrates containing different amounts of pore forming additive. With increasing amount of starch, the shrinkage of the anode substrate became greater. The anode substrate containing 30% starch shows the highest shrinkage after sinter-

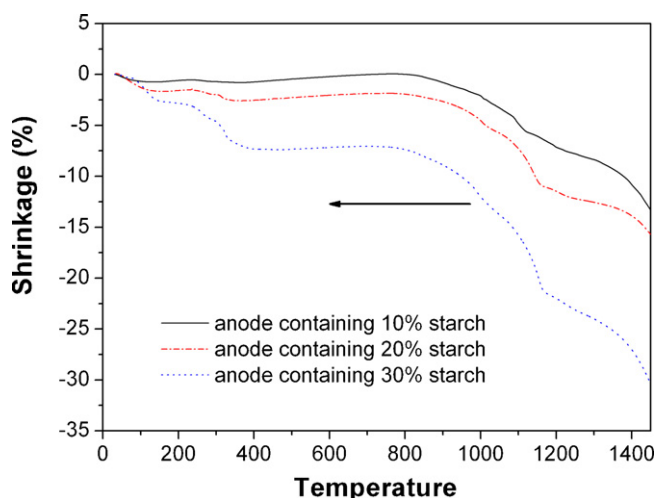


Fig. 1. Shrinkage of green anode substrates containing different amounts of starch.

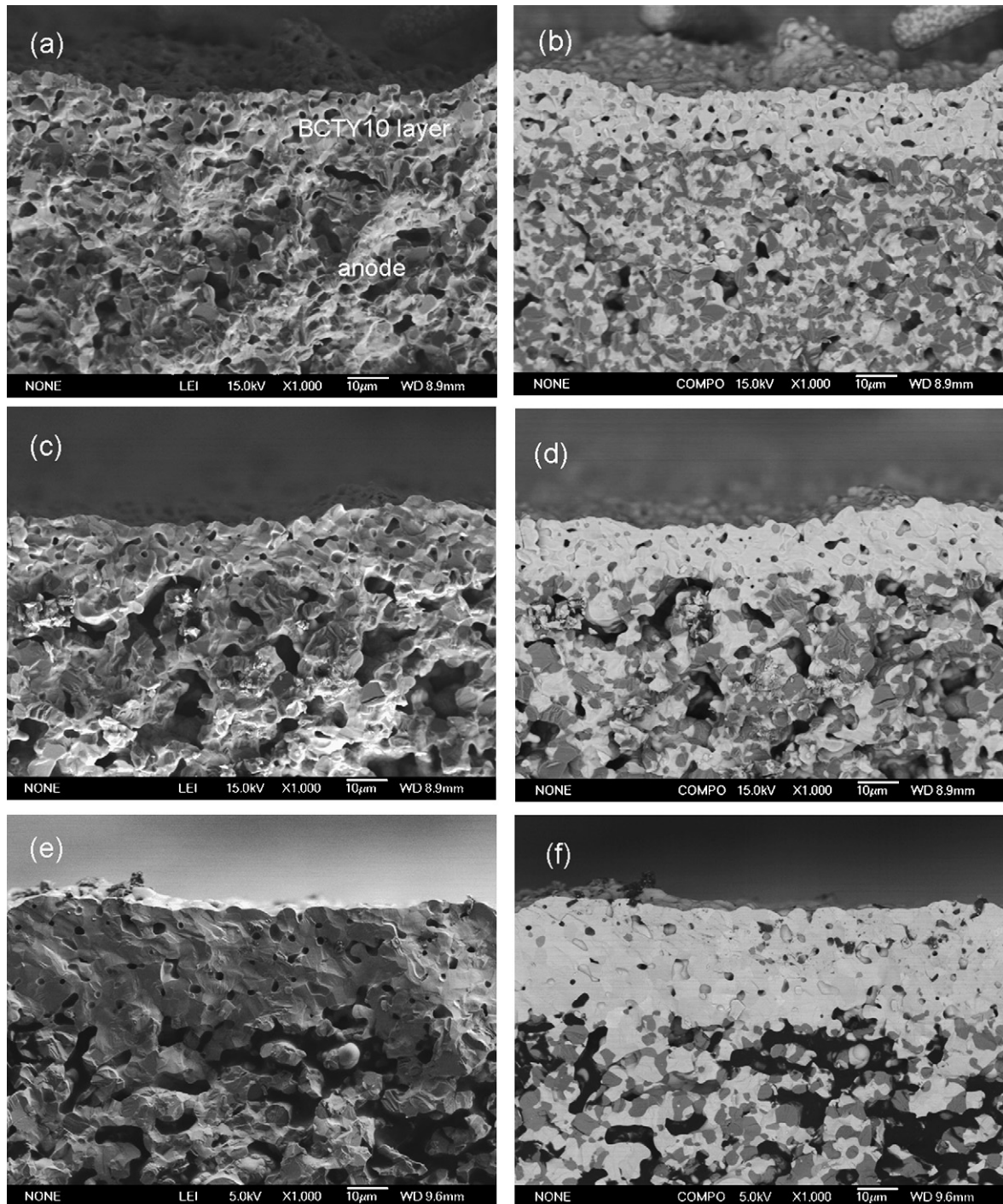


Fig. 2. Fracture surface of the half-cell based on a BCTY10 electrolyte membrane after sintering at 1450 °C. Secondary electron images of BCTY10 membranes on the anode substrates containing different amounts of starch (a) 10 wt.%, (c) 20 wt.% and (e) 30 wt.%. Backscattered electron images of the corresponding areas for (b) 10 wt.% starch containing anode, (d) 20 wt.% starch containing anode and (f) 30 wt.% starch containing anode.

ing at 1450 °C (~32.4%), which is beneficial to the densification of the membrane on this anode.

Fig. 2 presents cross-sectional views of the membranes prepared on the anode substrates containing different amounts of starch after sintering at 1450 °C for 5 h. Fig. 2(a), (c) and (e) are the secondary electron images of the fracture morphologies of the membranes on the anode substrates containing 10, 20 and 30 wt.% starch, respectively. Fig. 2(b), (d) and (f) are

the backscattered electron images of the corresponding areas of Fig. 2(a), (c) and (e), respectively. There is only one phase in the thin membranes as well as a good distribution of two phases in the anode substrates, implying that the pure phase ceramic membranes have been fabricated on the anode substrates. Furthermore, we can see from the SEM images that the membranes become denser with increasing amount of pore forming additive in the anode substrates. When 30 wt.% pore forming additive

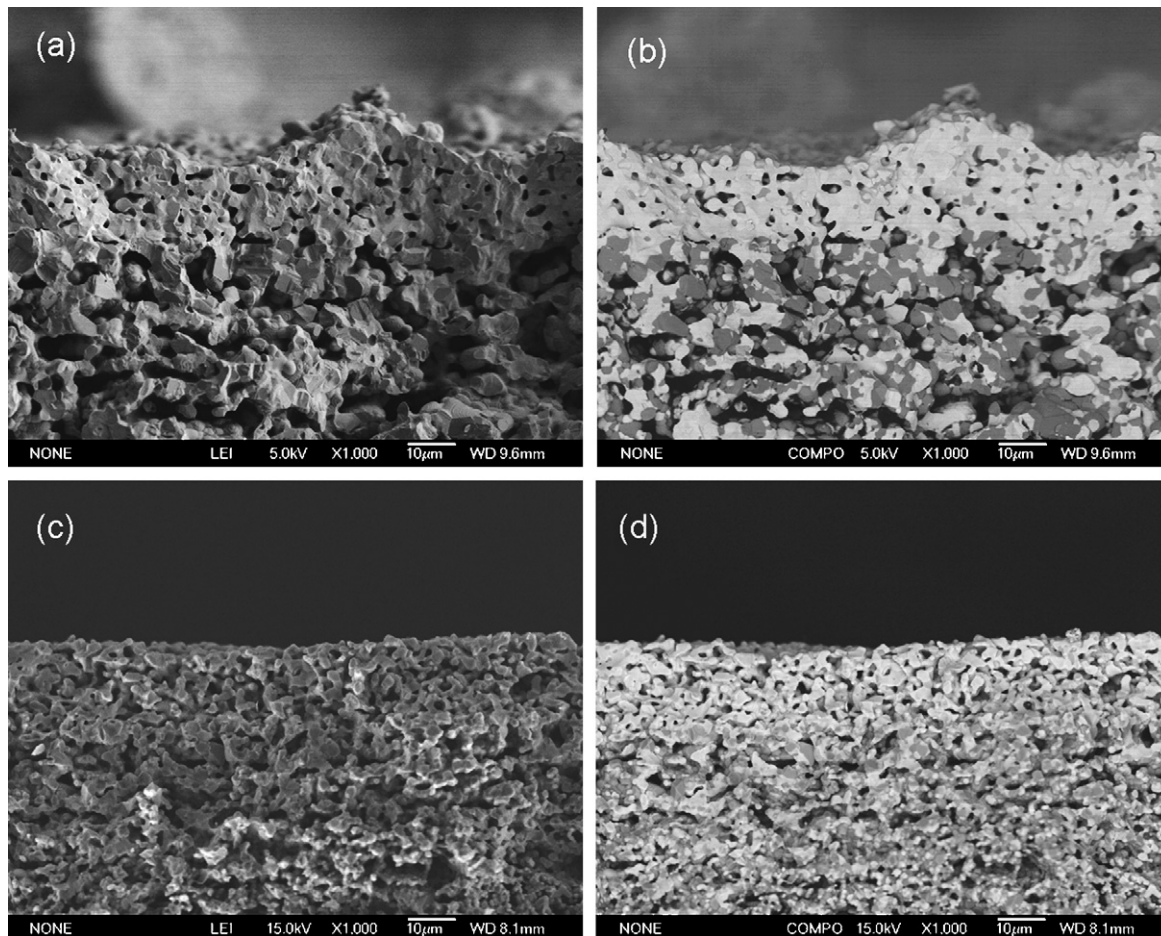


Fig. 3. Secondary electron image (a) and backscattered electron image (b) of the BCTY10 membrane on an anode substrate containing 30 wt.% starch after sintering at 1400 °C. Secondary electron image (c) and backscattered electron image (d) of the BCTY10 membrane on the 30 wt.% starch containing anode prepared by conventional powder solid state reaction after sintering at 1450 °C.

was added to the substrate, the membrane reached the highest density after sintering. For comparison, another two BCTY10 membranes were prepared using an in situ reaction but on different anode substrates. Fig. 3(a) and (b) shows images of a membrane on an anode containing 30 wt.% pore forming additive after sintering at 1400 °C for 5 h. We can see that the membrane was not dense even though 30 wt.% pore forming additive was added. This result implies that a sintering temperature of 1450 °C is required for the densification of BCTY10 membranes. Fig. 3(c) and (d) shows images of the membrane on an anode prepared by the conventional solid state powder reaction process after sintering at 1450 °C for 5 h, which also contained 30 wt.% pore forming additive in the anode. The membrane was not dense after sintering, indicating that the BCTY10 powder prepared by the conventional solid state reaction may not fit the requirement of fuel cell fabrication because of its low sintering activity. We also prepared a BCTY10 membrane on an anode substrate containing 40 wt.% pore forming additive. Though the membrane was dense after sintering, the poor mechanical property of the substrate especially after fuel cell testing made it difficult for general application. The results suggest that the dense BCTY10 membrane can be fabricated on the anode substrate in one step by optimizing the amount of pore

forming additive in the anode (30 wt.%) and using a sintering temperature of 1450 °C. It has to be mentioned that the sintering temperature of 1450 °C is slightly high for the manufacture of SOFCs, even though this sintering temperature is widely used for the fabrication of supported electrolyte membranes. Serra and co-workers^{10,17} have demonstrated that the sintering temperature of a supported electrolyte membrane can be reduced to 1300 °C by optimizing the anode substrate. Therefore, the optimization of the BCTY10–NiO anode substrate with reduction of the sintering temperature deserves further study.

In order to prove that the electrolyte membrane is the pure perovskite phase of BCTY10 and the anode has the expected composition of BCTY10 and NiO after sintering, XRD was used to examine the surfaces of the dense electrolyte membrane and the anode. Fig. 4(a) and (b) shows the XRD patterns of the anode and the membrane prepared by the in situ solid state reaction after sintering at 1450 °C for 5 h. The peaks all correspond to BCTY10 in the electrolyte membrane and to NiO and BCTY10 in the anode substrate, without any phases formed from other substances, indicating that the electrolyte membrane discussed above is the pure BCTY10 phase and the anode substrate indeed has the composition NiO–BCTY10. Although we directly mixed the metal oxides and metal carbonate for the anode substrates and

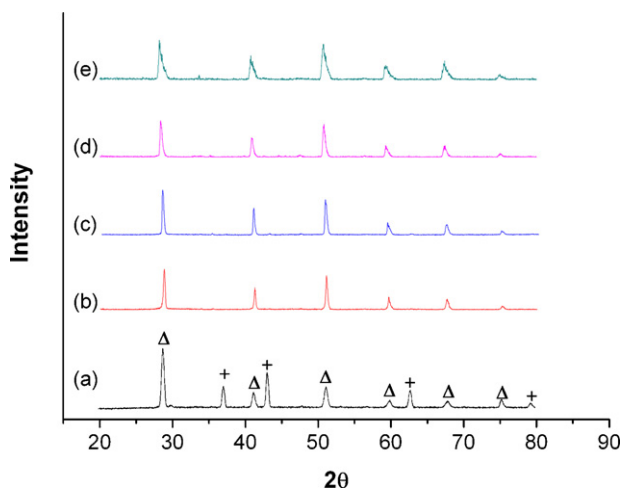


Fig. 4. XRD patterns for the bi-layers of (a) NiO–BCTY10 anode substrate, (b) BCTY10 membrane, (c) BCTY10 membrane after being boiled in water, (d) BCTY10 membrane after exposure to 100% CO₂ at 700 °C, (e) BCTY10 membrane after exposure to 100% CO₂ at 900 °C. (Δ) BCTY10; (+) NiO.

fired them together at a high temperature to produce BCTY10 and NiO, the XRD peaks of the BCTY10 in the anode shown in Fig. 4(a), shows no significant shift compared with the BCTY10 electrolyte membrane shown in Fig. 4(b). This result suggests that there is little incorporation of Ni into the BCTY10 lattice. According to a recent study,¹⁸ the incorporation of 1 mol.% Ni into a proton-conducting perovskite lattice is possible, which leads to improved sintering properties as well as a higher total electrical conductivity for the perovskite.

For this particular application the chemical stability of the BCTY10 membrane needs to be examined. The dense BCTY10 membrane was treated in boiling water as well as in 100% CO₂ at 700 and 900 °C. XRD examination of the sintered BCTY10 membrane after being boiled in water for 6 h, shown in Fig. 4(c), indicates that the BCTY10 remained unchanged, demonstrating that BCTY10 shows adequate stability against boiling water. As the BCTY10 electrolyte material is regarded as an electrolyte for an intermediate temperature SOFC, a stability test near the working temperature is necessary. We treated the dense BCTY10 membrane in a 100% CO₂-containing atmosphere with the flow rate of CO₂ set to 20 mL/min. Fig. 4(d) shows the XRD pattern of the BCTY10 membrane after exposure to 100% CO₂ at 700 °C for 3 h. We find that the BCTY10 remained unchanged, suggesting that BCTY10 shows adequate chemical stability in 100% CO₂ at 700 °C. Similarly, XRD examination of the BCTY10 membrane after exposure to 100% CO₂ at 900 °C for 3 h, shown in Fig. 4(e), indicates that the main structure of BCTY10 remained unchanged. However, the XRD peaks of BCTY10 become wider, which implies that the BCTY10 crystal begins to be destroyed after exposure to CO₂ at high temperature since the high temperature will increase the reaction rate. In spite of the wider peaks, no secondary phase can be observed in Fig. 4(e), indicating that the BCTY10 membrane shows reasonable stability in 100% CO₂, even at 900 °C.

To directly compare the influence on chemical stability between the Ta-doping strategy and the traditional Zr-doping

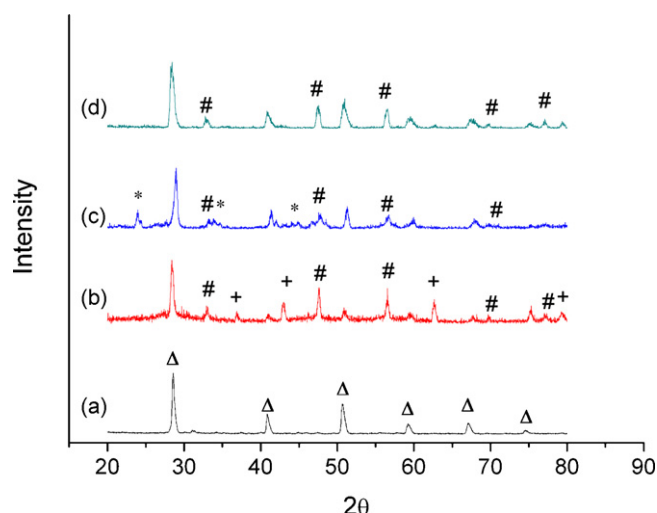


Fig. 5. XRD patterns of (a) BZCY7 membrane, (b) BZCY7 membrane after being boiled in water, (c) BZCY7 membrane after exposure to 100% CO₂ at 700 °C, (d) BZCY7 membrane after exposure to 100% CO₂ at 900 °C. (Δ) BZCY7; (+) NiO; (#) CeO₂; (*) BaCO₃.

strategy for BaCeO₃, a dense BaCe_{0.7}Zr_{0.1}Y_{0.2}O_{3-δ} (BZCY7) membrane prepared by the same method was also treated in boiling water and flowing CO₂. Fig. 5(a–d) is the XRD patterns of the dense BZCY7 membrane before and after being boiled in water or exposed to 100% CO₂ at 700 and 900 °C. The XRD pattern of a BZCY7 membrane after being boiled in water, shown in Fig. 5(b), suggests that the BZCY7 decomposes to Ba(OH)₂, CeO₂, ZrO₂ and Y₂O₃. It is difficult to distinguish ZrO₂ and Y₂O₃ in the XRD pattern as the amounts of these two compounds are too small. Furthermore, since the BZCY7 membrane is broken by attack from boiling water, the NiO in the anode is also reflected in the XRD pattern. The XRD pattern shown in Fig. 5(c) indicates that the BZCY7 decomposes to BaCO₃, CeO₂, ZrO₂ and Y₂O₃ during exposure to 100% CO₂ at 700 °C for 3 h. Fig. 5(d) presents the XRD pattern of a BZCY7 membrane after exposure to 100% CO₂ at 900 °C. Although no BaCO₃ peaks can be clearly observed in Fig. 5(d), due to the decomposition of BaCO₃ above 850 °C, the presence of the CeO₂ phase also suggests that the BZCY7 membrane decomposed during this treatment. The results directly indicate that the Ta-doped BaCeO₃ shows greater chemical stability than the commonly used Zr-doped BaCeO₃. The result also agrees well with that reported by Zhong.¹⁵ In his research, only a high proportion of Zr-doping (BaCe_{0.5}Zr_{0.4}Y_{0.1}O_{3-δ}) can make the BaCeO₃ materials adequately stable. In the present study, BCTY10 with only a small amount of Ta can make BaCeO₃ materials quite stable, implying that the partial replacement of Ce by Ta is a promising strategy for reaching a proper compromise between conductivity and chemical stability.

From the above discussion we know that the BCTY10 membrane on the anode containing 30 wt.% pore forming additive can meet the requirements for fuel cell testing, as the membrane was dense and stable. The development of proper cathode materials for SOFCs is an important task.^{19,20} For preliminary fuel cell testing, we used the LSF-BZCY7 composite material as a

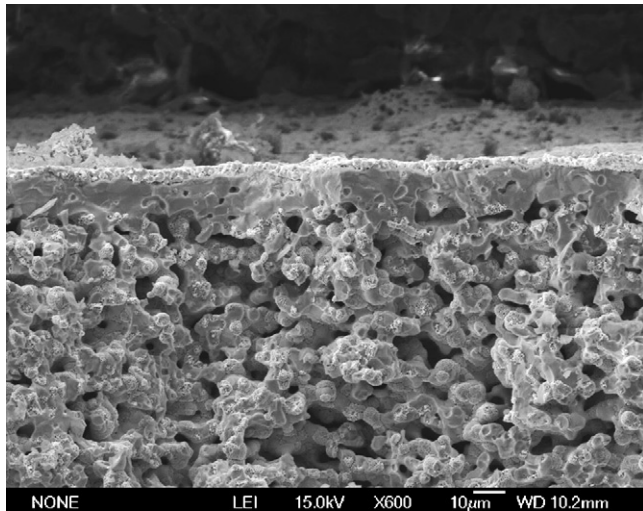


Fig. 6. SEM cross-sectional view of the single cell after testing.

cathode for the BCTY10-based fuel cell and the single cell was tested at different temperatures. Fig. 6 shows a typical scanning electron microscopy (SEM) image of the single cell after fuel cell testing. The SEM image indicates that the BCTY10 electrolyte membrane is 12 μm in thickness and is quite dense, without any connected pores and cracks after testing. Fig. 7 shows I - V and power density curves for a single cell based on a BCTY10 electrolyte membrane of 12 μm , measured at 500–700 $^{\circ}\text{C}$. The open circuit voltages (OCV) 0.997, 0.96 and 0.916 V at 500, 600 and 700 $^{\circ}\text{C}$, respectively, indicate that the BCTY10 electrolyte membrane is quite dense. With humidified hydrogen ($\sim 3\%$ H_2O) as the fuel and static air as the oxidant, maximum power densities of 29, 93, 142 mW/cm^2 were obtained at 500, 600 and 700 $^{\circ}\text{C}$, respectively. It has to be mentioned that we also used an Ag paste as a current collector for a BCTY10-based fuel cell, but the cell performance was lower than that of a fuel cell with a Pt paste as a current collector. This result suggests that Pt not only functions as a current collector but also plays the role of a catalytic layer for the oxygen. Though the BCTY10 electrolyte membrane was

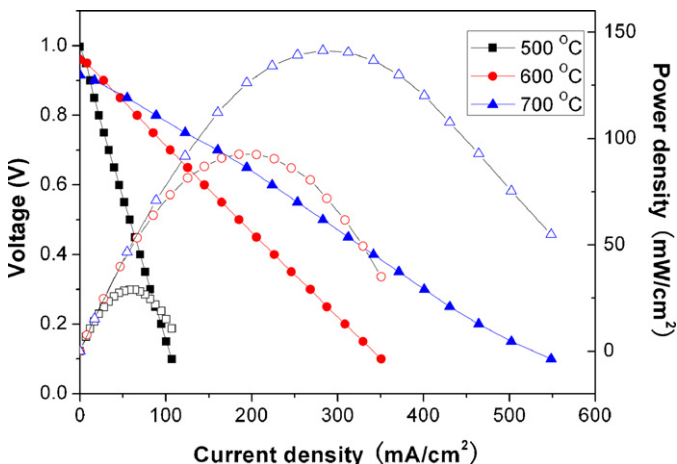


Fig. 7. Performance of a fuel cell with humidified hydrogen measured from 500 to 700 $^{\circ}\text{C}$.

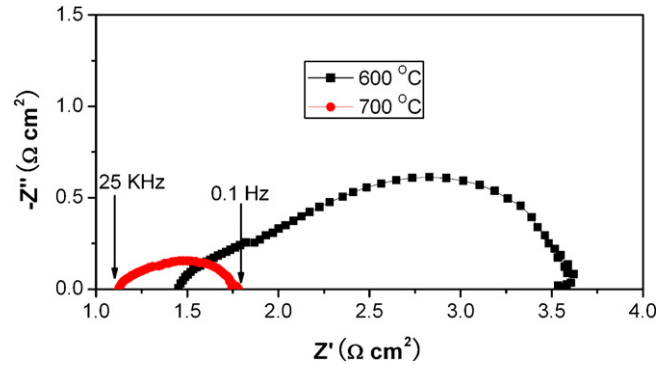


Fig. 8. Impedance spectra of a single cell measured under open circuit conditions at different temperatures.

only 12 μm thick and quite dense, the cell performance is not as high as we expected. There may be some factors restricting the cell performance.

Resistances of the cell under open circuit conditions were investigated by AC impedance spectroscopy. Two typical impedance spectra of the cell, measured at 600 and 700 $^{\circ}\text{C}$, are shown in Fig. 8. The intercept with the real axis at high frequency represents the overall electrolyte resistance including the ionic resistance of the electrolyte, the electronic resistance of the electrodes and some contact resistances associated with interfaces. On the other hand, the low frequency intercept corresponds to the total resistance of the cell. Therefore, the difference between the high frequency and low frequency intercepts with the real axis represents the total interfacial polarization resistance (R_p) of the cell. The overall electrolyte resistances of the cell are 1.45 $\Omega \text{ cm}^2$ at 600 $^{\circ}\text{C}$ and 1.12 $\Omega \text{ cm}^2$ at 700 $^{\circ}\text{C}$, while the R_p values are 2.09 $\Omega \text{ cm}^2$ at 600 $^{\circ}\text{C}$ and 0.65 $\Omega \text{ cm}^2$ at 700 $^{\circ}\text{C}$. Both the overall electrolyte resistance and the R_p are relatively high, which restricted the cell performance.

4. Conclusions

The half-cell with a structure consisting of a BCTY10 electrolyte membrane on a NiO-BCTY10 anode substrate was fabricated using a one step solid state reaction. After sintering at 1450 $^{\circ}\text{C}$, the BCTY10 membrane became dense only if the anode contained 30 wt.% starch. The stability tests showed that the BCTY10 membrane possessed adequate chemical stability against attack by H_2O and CO_2 . The power densities of the BCTY10-based fuel cell showed comparable performance to those of standard BaCeO_3 fuel cells. AC impedance studies indicated that the optimization of the cell structure deserved further study in order to achieve reduction of the relatively high overall electrolyte resistance and polarization resistance, both of which restricted the overall cell performance.

Acknowledgements

This work is supported by the National Natural Science Foundation of China (Grant nos.: 50602043 and 50730002).

References

1. Zuo, C. D., Zha, S. W., Liu, M. L., Hatano, M. and Uchiyama, M., Ba(Zr_{0.1}Ce_{0.7}Y_{0.2})O_{3-δ} as an electrolyte for low-temperature solid-oxide fuel cells. *Adv. Mater.*, 2006, **18**, 3318–3320.
2. Kreuer, K. D., Proton-conducting oxides. *Annu. Rev. Mater. Res.*, 2003, **33**, 333–359.
3. Iwahara, H., Uchida, H. and Morimoto, K., High-temperature solid electrolyte fuel-cells using perovskite-type oxide based on BaCeO₃. *J. Electrochem. Soc.*, 1990, **137**, 462–465.
4. Du, Y. and Nowick, A. S., Galvanic cell measurements on a fast proton conducting complex perovskite electrolyte. *Solid State Ionics*, 1996, **91**, 85–91.
5. Norby, T., Solid-state protonic conductors: principles, properties, progress and prospects. *Solid State Ionics*, 1999, **125**, 1–11.
6. Bi, L., Zhang, S. Q., Fang, S. M., Zhang, L., Xie, K., Xia, C. R. and Liu, W., Preparation of an extremely dense BaCe_{0.8}Sm_{0.2}O_{3-δ} thin membrane based on an in situ reaction. *Electrochem. Commun.*, 2008, **10**, 1005–1007.
7. Peng, R. R., Wu, Y., Yang, L. Z. and Mao, Z. Q., Electrochemical properties of intermediate-temperature SOFCs based on proton conducting Sm-doped BaCeO₃ electrolyte thin film. *Solid State Ionics*, 2006, **177**, 389–393.
8. Asamoto, M., Shirai, H., Yamaura, H. and Yahiro, H., Fabrication of BaCe_{0.8}Y_{0.2}O₃ dense film on perovskite-type oxide electrode substrates. *J. Eur. Ceram. Soc.*, 2007, **27**, 4229–4232.
9. Bi, L., Zhang, S. Q., Lin, B., Fang, S. M., Xia, C. R. and Liu, W., Screen-printed BaCe_{0.8}Sm_{0.2}O_{3-δ} thin membrane solid oxide fuel cells with surface modification by spray coating. *J. Alloys Compd.*, 2009, **473**, 48–52.
10. Serra, J. M., Buchler, O., Meulenber, W. A. and Buchkremer, H. P., Thin BaCe_{0.8}Gd_{0.2}O_{3-δ} protonic electrolytes on porous Ce_{0.8}Gd_{0.2}O_{1.9}-Ni substrates. *J. Electrochem. Soc.*, 2007, **154**, B334–B340.
11. Meulenber, W. A., Serra, J. M. and Schober, T., Preparation of proton conducting BaCe_{0.8}Gd_{0.2}O₃ thin films. *Solid State Ionics*, 2006, **177**, 2851–2856.
12. Leng, Y. J., Chan, S. H., Jiang, S. P. and Khor, K. A., Low-temperature SOFC with thin film GDC electrolyte prepared in situ by solid-state reaction. *Solid State Ionics*, 2004, **170**, 9–15.
13. Bi, L., Zhang, S. Q., Fang, S. M., Zhang, L., Gao, H. H., Meng, G. Y. and Liu, W., In-situ fabrication of a supported Ba₃Ca_{1.18}Nb_{1.82}O_{9-δ} membrane electrolyte for a proton-conducting SOFC. *J. Am. Ceram. Soc.*, 2008, **91**(11), 3806–3809.
14. Katahira, K., Kohchi, Y., Shimura, T. and Iwahara, H., Protonic conduction in Zr-substituted BaCeO₃. *Solid State Ionics*, 2000, **138**, 91–98.
15. Zhong, Z. M., Stability and conductivity study of the BaCe_{0.9-x}Zr_xY_{0.1}O_{2.95} systems. *Solid State Ionics*, 2007, **178**, 213–220.
16. Bi, L., Zhang, S. Q., Fang, S. M., Tao, Z. T., Peng, R. R. and Liu, W., A novel anode supported BaCe_{0.7}Ta_{0.1}Y_{0.2}O_{3-δ} electrolyte membrane for proton-conducting solid oxide fuel cell. *Electrochem. Commun.*, 2008, **10**, 1598–1601.
17. Serra, J. M. and Meulenber, W. A., Thin-film proton BaZr_{0.85}Y_{0.15}O₃ conducting electrolytes: toward an intermediate-temperature solid oxide fuel cell alternative. *J. Am. Ceram. Soc.*, 2007, **90**(7), 2082–2809.
18. Gorbova, E., Maragou, V., Medvedev, D., Demin, A. and Tsiakaras, P., Influence of sintering additives transition metals on the properties of gadolinium-doped barium cerate. *Solid State Ionics*, 2008, **179**, 887–890.
19. Zhang, H. Z. and Yang, W. S., Highly efficient electrocatalysts for oxygen reduction reaction. *Chem. Commun.*, 2007, 4215–4217.
20. Shao, Z. P. and Haile, S. M., A high-performance cathode for the next generation of solid-oxide fuel cells. *Nature*, 2004, **431**, 170–173.